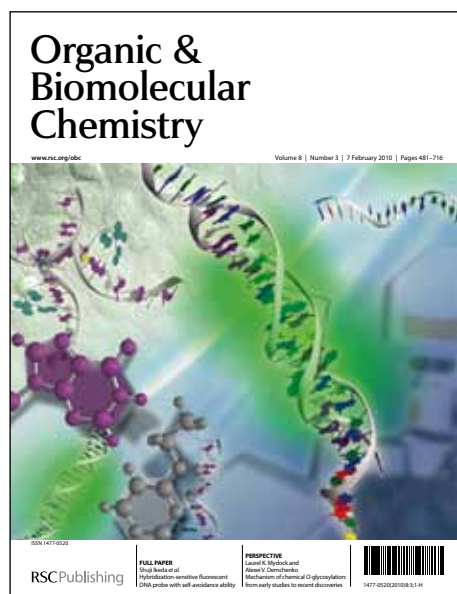


Organic & Biomolecular Chemistry

Accepted Manuscript



This is an *Accepted Manuscript*, which has been through the RSC Publishing peer review process and has been accepted for publication.

Accepted Manuscripts are published online shortly after acceptance, which is prior to technical editing, formatting and proof reading. This free service from RSC Publishing allows authors to make their results available to the community, in citable form, before publication of the edited article. This *Accepted Manuscript* will be replaced by the edited and formatted *Advance Article* as soon as this is available.

To cite this manuscript please use its permanent Digital Object Identifier (DOI®), which is identical for all formats of publication.

More information about *Accepted Manuscripts* can be found in the [Information for Authors](#).

Please note that technical editing may introduce minor changes to the text and/or graphics contained in the manuscript submitted by the author(s) which may alter content, and that the standard [Terms & Conditions](#) and the [ethical guidelines](#) that apply to the journal are still applicable. In no event shall the RSC be held responsible for any errors or omissions in these *Accepted Manuscript* manuscripts or any consequences arising from the use of any information contained in them.

Cite this: DOI: 10.1039/c0xx00000x

www.rsc.org/xxxxxx

ARTICLE TYPE

Molecular dynamics approaches to the design and synthesis of PCB targeting molecularly imprinted polymers: interference to monomer-template interactions in imprinting of 1, 2, 3-trichlorobenzene

Dougal Cleland,^a Gustaf D. Olsson,^b Björn C. G. Karlsson,^b Ian A. Nicholls^{b,c} and Adam McCluskey^{a*}⁵ Received (in XXX, XXX) Xth XXXXXXXXX 20XX, Accepted Xth XXXXXXXXX 20XX

DOI: 10.1039/b000000x

Abstract: The interactions between each component of the pre-polymerisation mixtures used in the synthesis of molecularly imprinted polymers (MIP) specific for 1,2,3,4,5-pentachlorobenzene (**1**) and 1,2,3-trichlorobenzene (**2**) were examined in four molecular dynamics simulations. These simulations revealed that the relative frequency of functional monomer-template (FM-T) interactions was consistent with results obtained by the synthesis and evaluation of the actual MIPs. The higher frequency of **1** interaction with trimethylstyrene (TMS; 54.7 %) than **1** interaction with pentafluorostyrene (PFS; 44.7 %) correlated with a higher imprinting factor (IF) of 2.1 vs. 1.7 for each functional monomer respectively. The higher frequency of PFS interactions with **2** (29.6 %) than TMS interactions with **2** (1.9 %) also correlated well with the observed differences in IF (3.7) of **2** MIPs imprinted using PFS as the FM than the IF (2.8) of **2** MIPs imprinted using TMS as the FM. The TMS-**1** interaction dominated the molecular simulation due to high interaction energies, but the weaker TMS-**2** resulted in low interaction maintenance, and thus lower IF values. Examination of the other pre-polymerisation mixture components revealed that the low levels of TMS-**2** interaction was, in part, due to interference caused by the cross linker (CL) ethyleneglycol dimethylacrylate (EGDMA) interactions with TMS. The main reason was, however, attributed to MeOH interactions with TMS in both a hydrogen bond and perpendicular configuration. This positioned a MeOH directly above the π -orbital of all TMS for an average of 63.8% of MD2 creating significant interference to π - π stacking interactions between **2** and TMS. These findings are consistent with the deviation from the 'normal' molecularly imprinted polymer synthesis ratio of 1:4:20 (T:FM:CL) of 1:20:29 and 6:15:29 observed with **2** and TMS and PFS respectively. Our molecular dynamics simulations correctly predicted the high level of interference from other MIP synthesis components. The effect on PFS-**1** interaction by MeOH was significantly lower and thus this system was not adversely affected.

30 Introduction

Molecularly imprinted polymers (MIP)s are robust synthetic materials designed for recognition, extraction and detection of specific target compounds.¹⁻¹⁰ MIPs have been developed for the detection of illicit drugs,^{11,12} environmental pollutants,² and for use in separation science.^{1,11-14}

Target specificity is imparted to MIPs at the synthesis stage where functional monomers (FM)s interact with the target (template) compounds (T), usually by non-covalent interactions such as hydrogen bonding, ion pairing and π - π -stacking interactions. These interactions result in the formation of a transient FM-T cluster creating a template specific binding cavity, that is locked by polymerisation in the presence of a cross linking agent (CL). Multiple polymerisation approaches have been examined; with bulk polymerisation dominating.¹⁵⁻²⁰ Subsequent removal of the template by exhaustive extraction releases a target specific binding site. The cross linker imparts structural rigidity and has been shown to be crucial for the

production of high quality MIPs.²¹ An alternative approach is to use a FM covalently attached to the target molecule. This covalent approach follows the same synthetic pathway as the non-covalent approach, but requires chemical cleavage of the FM-T bond to reveal the target specific binding sites. This increased synthetic requirement in conjunction with slow rebinding kinetics have led to the non-covalent MIP approach being the most prevalent.^{1, 13, 14, 21}

Polychlorinated biphenyls (PCB)s are classified as *persistent organic pollutants* requiring signatory countries of the Stockholm Convention to reduce and eliminate PCB containing equipment, prevent further release and monitor PCBs in the environment. PCB monitoring includes analysis of breast milk, foodstuffs as well as monitoring of sewage treatment plants and landfills suspected of having received PCB waste (including adjacent groundwater or leachate).²² The development of MIPs capable of recognising the PCB class of compounds, potentially offers an elegantly simple approach to future monitoring requirements by

detection, quantification and extraction of PCBs.

Crucial to the success of molecular imprinting, is the stability of the FM-T clusters formed within the pre-polymerisation mixture. The level of selectivity exhibited by a MIP has been directly related to the extent of these interactions.¹³ For a typical multi-functional template, such as caffeine,^{6, 7} propranolol^{8, 9} or homovanillic acid,¹⁰ these clusters are effectively stabilised by strong hydrogen bond or ion pair interactions, dependent on selection of a suitable FM and porogen. PCBs lack the appropriate functionality to associate with a FM by a strong hydrogen bond interaction and must associate with the FMs by relatively weak π - π stacking interactions. Imprinting of such poorly functionalised Ts by the non-covalent approach is a significant, and as yet, poorly addressed challenge for the development of MIPs.

In previous studies, techniques have been developed for the imprinting of poorly functionalised aromatic Ts. Baggiani *et al.* used suspension polymerisation to synthesise pyrene imprinted MIPs.²³ This involved injecting a standard pre-polymerisation mixture of pyrene, 4-vinylpyridine, divinylbenzene and chloroform, into a rapidly stirred solution of water, at 60 °C. Imprinting of pyrene was attributed to a combination of π - π stacking interactions and strong hydrophobic effects. Reddy *et al.*²⁴ and Kobayashi *et al.*²⁵ have both used the phase inversion technique to imprint dibenzofuran. This method involved mixing dibenzofuran with polysulfone in a hydrophilic solvent, dimethylacetamide. Water was then slowly added to the mixture while the polymers coagulated and encapsulated the dibenzofuran Ts. Yoshizako *et al.* developed PCB selective MIPs by polymerisation of ethyleneglycol dimethacrylate in a solution of xylene.²⁶ This method imparted a macro-porous structure to the polymers with selectivity for PCBs having similar structural arrangements as the porogen. Lübke *et al.* developed a semi-covalent approach to imprint MIPs with selectivity for polychlorinated dibenzodioxins (PCDD)s. This involved polymerisation of FMs covalently bound to the templates via cleavable urea bridges.²⁷ After synthesis, the FM-T linkages were hydrolysed and the Ts extracted. The binding sites synthesised by this approach retained amine functional groups optimally positioned to re-bind PCDDs via weak hydrogen bonds with the target chlorine substituents.

Our approach to the synthesis of PCBs selective MIPs has involved the development of a simple, robust and reliable non-covalent method utilising π - π stacking interactions with aromatic FMs. We examined the potential of these interactions to imprint chlorinated aromatic templates by an Effective Fragment Potential (EFP) molecular modelling study.²⁸ This technique highlighted high levels of favourable interactions between aromatic templates and the FMs evaluated (styrene (STY), 2, 4, 6-trimethylstyrene (TMS), 2, 3, 4, 5, 6-pentafluorostyrene (PFS) and 4-vinyl pyridine (4VP)). These FMs have afforded access to MIPs selective for 1, 2, 3, 4, 5-pentachlorobenzene (**1**) and 1, 2, 3-trichlorobenzene (**2**) and their subsequent use as fragment imprinting surrogates for selected PCBs and confirmed the feasibility of our approach. However, the weak π - π stacking interactions resulted in low stability of the FM-T clusters and even a weak interaction with another component of the pre-polymerisation mixture had the potential to adversely affect the specificity of the synthesised MIPs. Methanol (MeOH) was used as the porogen in these studies as it presented the best compromise between solvophobic properties and pre-polymerisation cluster component solubility, but as our EFP studies demonstrated, MeOH had significant potential to form unfavourable interactions with the other pre-polymerisation

cluster components. Notwithstanding this, we applied an extreme vertices mixture design (EVMD) chemometric approach to post design optimisation of MIP specificity. This led to the rapid development of high efficacy MIPs for **2** with IF values of 2.8 with TMS as FM in a FM: T: CL ratio of 20:1:29 and IF values of 3.7 with PFS as FM in a FM: T: CL ratio of 15:6:29.²⁹ In these latter studies it was apparent that imprinting of **2** was not solely due to the EFP predicted FM-T interactions. We were unable to evaluate the interactions between the cross linker, EGDMA, as in an EFP simulation the internal geometries of the molecules remain fixed. This is suitable for small solvent molecules or rigid aromatic molecules, but not so case for highly flexible molecules, such as EGDMA. Despite providing accurate values for the FM-T interactions, the EFP approach failed to predict this less favourable (low levels of imprinting) outcome with **2**. Further investigation using our EFP approach was not feasible due to the increased complexity of the data set required to evaluate the true nature of the MIP pre-polymerisation cluster component interactions. Kaliman and Slipchenko have recently reported a parallel implementation of the EFP approach, and in this study conducted a molecular dynamics simulation of 216 water molecules for 1 ns.³⁰ The accurate theoretical description of polyfunctional, multi component systems remains a major challenge in computational chemistry. Even with the advances in computer power, descriptions of systems beyond 10-100 atoms at the high levels of theory required to examine the type of interaction we have noted with aromatic systems is not currently feasible. Thus while our prior studies demonstrated that the imprinting of PCBs was clearly feasible, the exact nature of the favourable imprinting was not determined.

We have previously used a molecular dynamics approach to evaluate non-covalent interactions within the synthetic formulation of a MIP, but these studies were limited to systems displaying high levels of hydrogen bonding interactions.³¹⁻³⁴ This approach permits the qualitative prediction of the types of interactions within a mixture as well as the frequency and lifetimes of such interactions across a given time frame. Previous studies have furnished detailed insights and provided potential explanations for the binding site heterogeneity observed in MIPs³¹ and the role of the CL in imprinting of Ts.³²⁻³⁵ Herein, we report the application of molecular dynamics simulations in the evaluation of FM interactions within the pre-polymerisation mixtures used for the synthesis of PCB selective MIPs. These studies were conducted using 1,2,3,4,5-pentachlorobenzene (**1**) and 1,2,3-trichlorobenzene (**2**) as PCB surrogates (Figure 1) and also as surrogates for other poorly functionalised MIP templates such as the chlorinated herbicides.³⁶

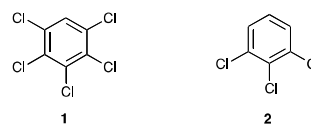


Figure 1. Chemical structures of the PCB surrogate templates, 1, 2, 3, 4, 5-pentachlorobenzene (**1**) and 1, 2, 3-trichlorobenzene (**2**).

115 Results and Discussion

Our earlier EFP studies specifically targeted computation of the energy of interactions between those components whose composition changed between each of the MIP synthesis protocols, the FM and T. In doing so EFP identified four aromatic FMs capable of forming π - π stacking interactions with the templates **1** and **2** (Figure 2).²⁸ With **1** the interaction energy increased in rank order from PFS (8.7 kcal mol⁻¹) < 4VP (10.7 kcal mol⁻¹) < STY (11.7 kcal mol⁻¹) < TMS (12.9 kcal mol⁻¹) and

with **2** from PFS ($9.0 \text{ kcal mol}^{-1}$) < 4VP ($9.6 \text{ kcal mol}^{-1}$) = STY ($9.6 \text{ kcal mol}^{-1}$) < TMS ($10.8 \text{ kcal mol}^{-1}$). These data suggested, for both templates, that TMS was the most promising FM for imprinting. Subsequent synthesis and evaluation of the MIPs revealed that TMS was the optimal FM for the synthesis of a **1** selective MIP, as predicted by the interaction energy and the optimum proportions were 1: 2: 10 (T: FM: CL) and resulted in an IF = 2.1.²⁸ The optimum FM for the synthesis of a **2** selective MIP was however PFS, contradicting the EFP interaction energy based prediction. In this instance the optimum proportions for MIP_{2-PFS} were 15: 6: 29 (T: FM: CL) which returned an IF = 3.7 and for MIP_{2-TMS} were 20: 1: 29 (T: FM: CL) which returned lower IF = 2.8.²⁹ These results while showing specific recognition of the parent template strongly suggested that TMS had not interacted with **2** to any significant degree. The deviation from the typical FM: T: CL ratio also suggested that the observed specificity was not a direct result of strong FM: T interactions. Logically the poor outcome associated with MIP_{2-TMS} was a result of competing interactions with other pre-polymerisation mixture components.

As in all MIP synthesis, the porogen (herein MeOH) constitutes the major component of the pre-polymerisation mixture, and thus logically the most likely component to adversely affect the interaction of **2** with TMS. MeOH was chosen as porogen as, of all the potential porogens examined, it displayed the most favourable combination of solvophobic properties and solubility for the pre-polymerisation components.²⁸ The porogen solvophobic properties relate to the propensity of the porogen to encourage micelle formation of the non-soluble (or sparingly soluble) components of the pre-polymerisation cluster. Here porogens that allow full dissolution of the FM, T and CL do so by disruption of the cohesive forces between the porogen molecules. A highly solvophobic porogen resists perturbation of its cohesive forces. In a highly solvophobic solvent the non-soluble components self-associate and with the synthesis of the MIPs described herein, the augments the interaction between the key pre-polymerization cluster components potentially enhancing the lifetime of the pre-polymerization cluster and potentially creating higher affinity binding sites.

The application of a solvophobic effect in any MIP synthesis is ultimately a compromise with the porogen required to retain high internal cohesiveness while dissolving a small proportion of the pre-polymerization cluster components (or the polymerization would most likely be heterogeneous). Thus any solvent that enhances component solubility, by default reduces the solvophobic effects. In our initial studies we examined the effect of changing porogen (CH₂Cl₂, CH₃CN and MeOH) on the IF (1.0, 1.0-1.1 and 1.3-2.3 respectively) of the resultant MIPs with the outcomes noted in Table 1. With increasing component solubility (decreasing solvophobic effect) we noted a loss of imprinting (c.f. Table 1 entry 5 and 1). This is consistent with the porogen solvophobic properties enhancing the lifetime and strength of the FM-T interactions, in turn affording higher affinity binding sites in template removal. The use of MeOH has previously been shown to decrease unfavorable self-association of key pre-polymerisation cluster components reducing non-specific binding, and this may have played a role in the increased specific binding noted with **1** and **2** using MeOH as the porogen.^{37,38}

Table 1: Factors modified in the synthetic procedure towards TMS based selective MIPs selective for **1** and the experimentally derived IF values.

Entry	Proportions (T: FM: XL)	Porogen	Initiation	IF
1	1: 4: 20	CH ₂ Cl ₂	Thermal	1.0
2	1: 4: 20	MeCN	Thermal	1.0
3	1: 4: 20	MeCN	UV	1.1
4	1: 4: 20	MeOH	UV	1.3
5	1: 2: 10	MeOH	UV	2.1

Given the increase specificity noted with the MIPs synthesized in MeOH, we attempted to enhance the solvophobic effect of methanol through the addition of H₂O, but this resulted in reducing the component(s) solubility and with the effect of reducing the observed imprinting factor.

Subsequent calculation of the energy of interaction of MeOH with the FMs showed that the strength of these interactions increased, in rank order, from STY ($4.9 \text{ kcal mol}^{-1}$) < PFS ($5.4 \text{ kcal mol}^{-1}$) < TMS ($6.1 \text{ kcal mol}^{-1}$) < 4VP ($6.7 \text{ kcal mol}^{-1}$). This suggested that 4VP was the FM most susceptible to interference caused by interactions with MeOH. Although TMS had relatively strong interaction energy with MeOH, TMS had much stronger interaction energy with **1** and **2** than 4VP, and this was initially predicted to offset the possible deleterious effect of the aforementioned interaction with MeOH. Ethyleneglycol dimethacrylate (EGDMA) was used as CL.

To gain a better insight into the possible interactions (favourable and unfavourable), and thus an explanation of our results with TMS and PFS, we employed a molecular dynamics approach to examine potential interactions within the MIP synthesis pre-polymerisation cluster. Four molecular dynamics simulations, MD1-MD4 (Table 2), were conducted as described in the experimental section. On completion, the average spatial distribution of all pre-polymerisation components were extracted from the trajectories by calculation of the radial distribution function (RDF). From a RDF, non-covalent interactions with the FMs during the simulations were identified by an increase in the density of a pre-polymerisation component at an energy optimised distance from the FMs. For the FM-T and FM-solvent interactions these distances were compared to the energy optimised distances calculated in our EFP study (ESI Figure S1).

Table 2. Composition of the molecular dynamics simulations showing the numbers in parentheses and types of components used in these molecular dynamics simulations.

Simulation	Template	Functional Monomer	Cross-Linking Monomer	Porogen
MD1	1 (31)	TMS (125)	EGDMA (500)	MeOH (2468)
MD2	2 (31)	TMS (125)	EGDMA (500)	MeOH (2468)
MD3	1 (31)	PFS (125)	EGDMA (500)	MeOH (2468)
MD4	2 (31)	PFS (125)	EGDMA (500)	MeOH (2468)

Functional Monomer – Template Interactions

Unlike hydrogen bond interactions between a typical FM and template that take place in a well defined configuration and can be evaluated by calculation of a single RDF between the hydrogen bond donor and acceptor atoms, aromatic systems are more complex. π - π stacking interactions can potentially occur in a number of different orientations.^{39,40} To ensure that all interactions were accounted for, a RDF was calculated between each symmetrically unique aromatic carbon of the FMs (C1-C4)

and each symmetrically unique aromatic carbon of the templates (C1-C4) (Figure 2).

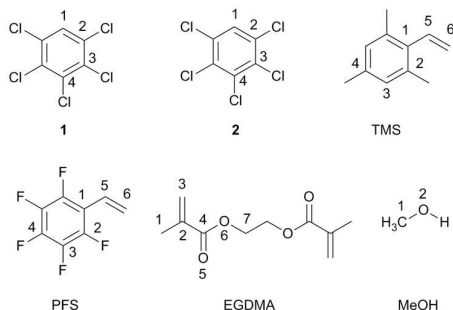


Figure 2. Chemical structures and unique atom identifiers for molecules examined by molecular dynamics simulations (indicated by the addition of a number next to the appropriate atom): 1, 2, 3, 4, 5-pentachlorobenzene (**1**); 1, 2, 3-trichlorobenzene (**2**); 2, 4, 6-trimethylstyrene (TMS); 2, 3, 4, 5, 6-pentafluorostyrene (PFS); (C); ethyleneglycol dimethacrylate (EGDMA); and MeOH.

10 Template 1 - TMS Interactions

Of the MIP systems evaluated for **1** and **2**, both calculation and batch rebinding indicated that the strongest π - π stacking interactions were between TMS and **1** this is examined in MD1 (Table 1). Our EFP analysis predicted a favourable interaction between C1 of **1** ($\mathbf{1}_{C1}$) and C1 of TMS (\mathbf{TMS}_{C1}) which correlated well with the observed RDF peak maximum for this interaction at 3.8 Å. The RDF shows a well defined first peak in the density of $\mathbf{1}_{C1}$ at 3.8 Å followed by a second broader peak in the radial distribution density between 7.5 and 9.5 Å, most probably due to formation of a stacked structure incorporating multiple molecules of **1** (Figure 3). Moreover the data extracted from all RDFs calculated between **1** and TMS showed a peak density of all **1** atoms, for all possible permutations of a π - π stacking interaction between **1** and TMS, at distances of between 3.8 and 4.0 Å from the TMS atoms. The presence of a RDF peak density at a similar distance from all TMS atoms was consistent with π - π stacking in multiple orientations, which had aligned each **1** atom with each TMS atom. Integration of the RDFs calculated that 0.547 **1** were in π - π stacking interactions with TMS for the duration of the simulation time for MD1. We interpreted this as indicating that, on average, all **1** were in a π - π stacking interaction with a TMS for 54.7 % of the simulation time for system MD1, in agreement with previous results obtained from EFP predictions.²⁸

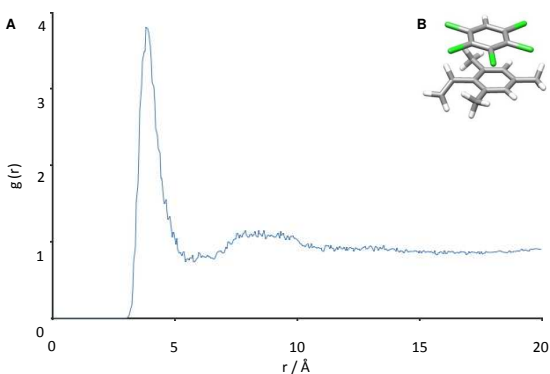


Figure 3. (A) RDF showing the density of $\mathbf{1}_{C1}$ as a function of the distance from \mathbf{TMS}_{C1} during MD1. (B) The EFP predicted geometry of FM-T interaction between **1** and TMS.²⁸

Template 2-TMS Interactions

The interactions of **2** with TMS during MD2 afforded RDFs with small broad maximums in the densities of $\mathbf{2}_{C1}$ and $\mathbf{2}_{C2}$

between 4.0 and 5.0 Å from the TMS atoms. These broad increases in the density however lacked the sharp peak typically associated with non-covalent interactions.^{33,34} Larger peaks in the densities of $\mathbf{2}_{C3}$ and $\mathbf{2}_{C4}$ were also detected between 5.9 and 6.4 Å from the TMS atoms (Figure 4). Although these larger increases in the density suggested there was an accumulation of **2** in the proximity of TMS the distance to these peaks was much larger than the separation between atoms in a typical non-covalent interaction, suggesting a degree of non-specific interaction, and not the favourable interactions predicted by EFP calculations.

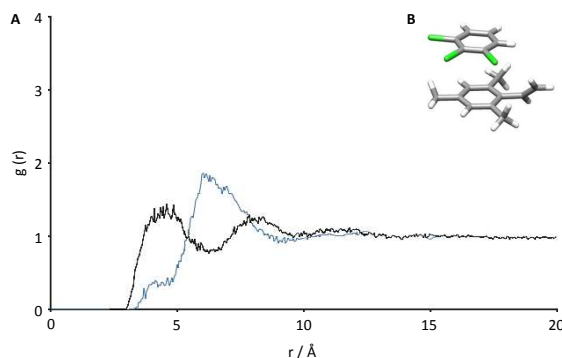


Figure 4. (A) RDFs showing the density of **2** atoms as a function of the distance from TMS atoms during MD2: $\mathbf{2}_{C1}$ - \mathbf{TMS}_{C1} (— trace) and $\mathbf{2}_{C4}$ - \mathbf{TMS}_{C4} (--- trace). (B) The EFP predicted geometry of FM-T interaction between **2** and TMS.²⁸

The examination of this RDF only accounted for the parallel facial π - π interaction as shown in Figure 4B. However, aromatic molecules often interact in T-shape configurations which are favoured in a dynamic system as they do not restrict the motion of the interacting molecules to the same extent as the parallel facial π - π interactions and consequently reduce the entropic penalty of association. Although we did not identify a T-shaped interaction between **2** and TMS by EFP calculation, it was conceivable that this static modelling snapshot failed to accurately describe and capture all relevant interactions. In a T-shape configuration aromatic compounds orient perpendicular to one another with the hydrogen of one compound directed toward the π -orbital of the other compound. The strength of these interactions increase when the axially disposed compound contains a *para*-electron withdrawing moiety (to the interacting hydrogen atom), e.g. the Cl of **2**; and the facial compound has an electron donating substituent, e.g. CH_3 moieties of TMS.³³ Accordingly in the most probable T-shape configuration, **2** would adopt an axial disposition with TMS facially positioned (ESI Figure S2). To examine the possibility of such a T-shape interaction, RDFs were calculated between $\mathbf{2}_{\text{HI-H2}}$ and \mathbf{TMS}_{C1-C4} . These RDFs showed small peaks in the densities of $\mathbf{2}_{\text{HI}}$ atoms between 2.9 and 3.1 Å from \mathbf{TMS}_{C1-C4} (ESI Figure S3). These distances can be associated with a T-shaped configuration. Integration of these peaks however revealed that all $\mathbf{2}_{\text{HI}}$ were within 3.1 Å of a \mathbf{TMS}_{C1} for an average of only 1.9% of MD2. Overall this lack of **2**-TMS interaction was contrary to our EFP findings, but consistent with the poor IF value observed on synthesis and evaluation of the subsequent MIP_{2-TMS}. It again suggests that the observed IF for MIP_{2-TMS} was not a consequence of pre-polymerisation cluster associations between the FM and T.

Template 1-PFS Interactions

Similar evidence for π - π stacking interactions between **1** and PFS in MD3 was observed as previously identified for **1** and TMS in MD1. This was evident from the large first peak in the densities of all $\mathbf{1}_{C1-C4}$ within 3.7 and 4.0 Å from all \mathbf{PFS}_{C1-C4}

atoms (Figure 5). The distance to the closest peak in the densities of **1** atoms with PFS at 3.7 Å was marginally closer than observed in the presence of TMS at 3.8 Å. RDFs accounting for all **1** atom peaks were observed as having maxima in the 3.7–4.0 Å range again consistent with the π - π interactions occur in multiple orientations, and with our EFP results.²⁸ These π - π stacking interactions during MD3 suggested that PFS would facilitate imprinting of **1** which is consistent with the results obtained by the synthesis and evaluation of the MIPs. A second smaller peak in the RDF was observed at 7.0 Å suggesting an accumulation of **1**_{C4} in the vicinity of PFS_{C1}. The extent of interactions between **1** and PFS was calculated, and on average all **1** were in a π - π stacking interaction with a PFS for 44.7% of MD3, marginally less than the 54.7% interaction calculated in MD1.

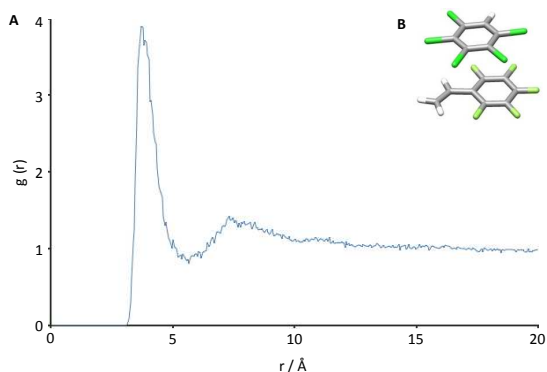


Figure 5. (A) RDF showing the average density of **1**_{C4} as a function of the distance from PFS_{C1} during MD3. (B) The EFP predicted geometry of FM-T interaction between **1** and PFS.²⁸

20 Template 2-PFS Interactions

The RDFs calculated between **2** and PFS strongly suggested that π - π stacking interactions had taken place during MD4 with observation of peaks in the densities of all **2** atoms between 3.7 and 4.0 Å from all PFS atoms (Figure 6). These peaks in the densities of **2** atoms were less pronounced than the peaks in the densities of **1** atoms in the presence of PFS with each **2** in a π - π stacking interaction with a PFS for an average of 29.6% of MD4. This is 66% of the calculated PFS-**1** frequency of interaction. Importantly, the interactions of **2** with PFS were identified in a π - π stacking configuration that was not observed in the presence of TMS. This was consistent with the improved IF values for MIP_{2-PFS} (3.7) versus MIP_{2-TMS} (2.8). From these results, it appeared that the molecular dynamics simulations had accurately reproduced the competing interactions within the pre-polymerisation mixtures for **2** imprinted MIPs. This result was unexpected as the EFP calculated interaction energy of **2** with TMS at 10.8 kcal mol⁻¹ was higher than that of **2** with PFS at 9.0 kcal mol⁻¹. The **2**-TMS interaction is 2.1 kcal mol⁻¹ less favourable than the **1**-TMS interaction. This most likely positions the **2**-TMS interactions more susceptible to unfavourable interactions within the pre-polymerisation mixture and this is evidenced by the lower frequency of interactions of **2** with TMS.

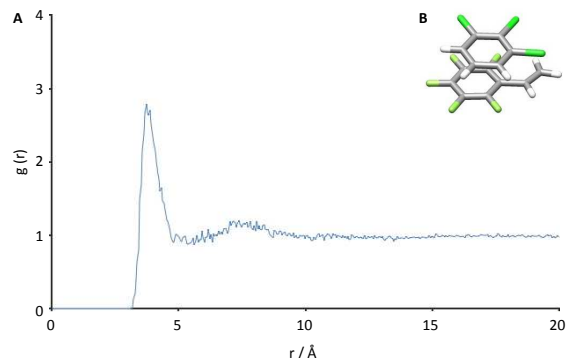


Figure 6. (A) RDF showing the density of **2**_{C4} as a function of the distance from PFS_{C1} during MD4. (B) The EFP predicted geometry of FM-T interaction between **2** and PFS.²⁸

Competing Interactions – FM-FM Interactions

Having demonstrated that the molecular dynamics simulations were consistent with the predicted FM-T interactions and outcomes of subsequent MIP evaluations for **1**-TMS, and also with **2**-TMS (unlike our EFP study), we applied the MD approach to the examination FM-FM, FM-CL and FM-solvent interactions. These evaluations were limited to MD2 and MD4 (Table 1), as these systems showed the largest divergence in outcomes, in an effort to determine which factors adversely affected the MIP specificity. **1**-CL and **2**-CL interactions were evaluated during MD3 and MD4. Although these final interactions competed for template-FM interactions they were predicted to increase MIP specificity as suggested by previous studies.^{31,33,34}

FM-FM self-association was anticipated to occur in a π - π stacking configuration. The RDFs for TMS-TMS (MD2) interactions showed small peaks in the density of TMS_{C1-C4} between 6.0 and 6.2 Å from TMS_{C1} (ESI Figure S4). These interactions were comparable with the increases in density of TMS atoms observed in the presence of **2**. These peaks in the density of TMS atoms did not suggest that interactions had occurred in a π - π stacking configuration, c.f. **2** and TMS. To further analyse TMS self-association an additional RDF was calculated between TMS_{H3} and TMS_{C1} (ESI Figure S5). This was conducted to determine if interactions had taken place in a T-shaped configuration. Similar to the RDFs between **2**_{H1} and TMS_{C1-C4} a small peak in the densities of TMS_{H3} was observed 3.0 Å from TMS_{C1}. Integration of this peak however revealed that all TMS_{H3} were within 3.3 Å of a TMS_{C1} for an average of only 1.2% of MD2. This indicated that if interactions in a T-shaped configuration had transpired they were at most infrequent and unlikely to cause significant interference to TMS interactions with **2**.

For PFS, a sharp peak in the density of PFS_{C1-C4} atoms between 3.7 and 4.0 Å from PFS_{C1} was consistent with a π - π stacking interaction and PFS-PFS self-association occurring for an average of 21.5% of MD4 (ESI Figure S6). This is equal to the estimated frequency of PFS interactions with **2** (above). The persistent self-association of PFS would have most likely reduced the frequency of PFS interactions with **2**. PFS interactions with **2** were however commonplace whereas TMS, which was not observed to significantly self-associate, lacked interactions with **2**. This suggests that while FM self-association might reduce the frequency of interactions with **2** it clearly did not prevent them. Nevertheless this would be expected to adversely affect crucial pre-polymerisation cluster interactions. No such TMS-TMS interaction was observed.

Competing Interactions – Porogen - FM Interactions

From the EFP calculated interaction energy the most probable

interactions were between a lone pair electron orbital of the MeOH oxygen and the π -orbital of PFS (ESI Figure S1) and a hydrogen bond with the π -orbital of TMS (Figure 7B). A RDF calculated between MeOH_{O2} and PFS_{C1}, failed to reveal any increase in the density of MeOH in proximity to PFS indicating a complete lack of interactions. In contrast small peaks in the density of MeOH_{H2}, MeOH_{O2} and MeOH_{C1} were observed 2.5, 3.4 and 3.8 Å from TMS_{C1}. These first peaks in the density were followed by second larger increases in the density of MeOH atoms which were attributed to a layered structure of MeOH solvating the TMS (Figure 7A).

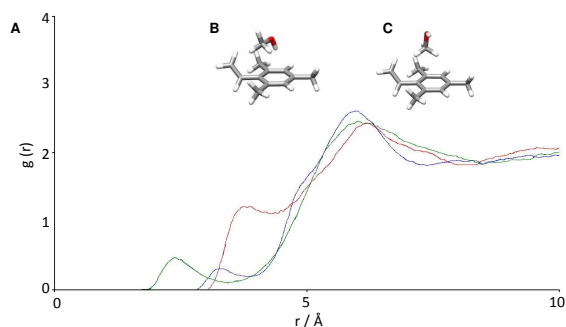


Figure 7. (A) RDFs showing the density of MeOH atoms as a function of their distance from TMS_{C1} during MD2. MeOH_{H2}-TMS_{C1} (— trace), (B) MeOH_{O2}-TMS_{C1} (— trace) and MeOH_{C1}-TMS_{C1} (— trace). (B) EFP optimised configuration of MeOH with TMS in a hydrogen bond configuration; and (C) MeOH in a perpendicular configuration with TMS.²⁸

The distances to the first peaks in the densities implied that interactions had transpired in a hydrogen bond configuration by the similarity to the inter-molecular separations measured in the EFP optimised configuration. Integration of these peaks revealed that on average all MeOH_{H2} were within 3.0 Å of a TMS_{C1} for 9.4 % of MD2, and this was reasonably consistent with the results for MeOH_{O2} which was within 4.0 Å of a TMS_{C1} for 12.9 % of MD2. Integration of the peak in the density of MeOH_{C1}, however, revealed that all MeOH_{C1} were within 4.2 Å of a TMS_{C1} for an average of 63.8 % of MD2. This result suggested that another interaction was, in part, responsible for the large peak in the density of MeOH_{C1} 3.7 Å from TMS_{C1}. This interaction was proposed to be the perpendicular configuration identified (Figure 7C). In the EFP optimised configuration of a perpendicular configuration the MeOH_{C1} is 3.5 Å from TMS_{C1} which correlated well with the distance to the first peak in the density of MeOH_{C1} atoms (3.7 Å). In addition, an interaction in this configuration would increase the size of the first peak in the density of MeOH_{C1} without affecting the first peak in the densities of MeOH_{O2} and MeOH_{H2}. Importantly, any combination of interactions that positioned a MeOH directly above the TMS for an average of 63.8 % of MD2 would have caused significant interference to TMS interactions with **2** during MD2.

Competing Interactions – CL-FM Interactions

Due to the lack of suitable functionality, EGDMA was not expected to form strong non-covalent interactions with the aromatic carbon of the FMs with exception of potential interaction between a lone pair electron orbital of an EGDMA carbonyl oxygen and the electron deficient π -orbital of PFS. Similar interactions have been predicted by high level theoretical calculations between water and the electron deficient π -orbital of 1,2,4,5-tetracyanobenzene.³⁴ The most probable interactions were anticipated to be hydrogen bond interactions between either PFS_{H5-H6} or TMS_{H3-H5-H6} and the carbonyl oxygen of EGDMA.

Similar interactions with EGDMA have been predicted by previous molecular dynamics studies.³²

From calculated RDFs evaluating the accumulation of EGDMA around PFS, small peaks in the density of EGDMA_{O5} 2.8 Å from PFS_{H5} and 2.9 Å from PFS_{H6} suggested that hydrogen bond interactions had ensued during MD4 (ESI Fig. S7). Similar peaks were observed in the density of EGDMA_{O5} 2.8 Å from TMS_{H3-H5-H6} (ESI Fig. S8). It is difficult to predict the level of interference these interactions might cause to FM interactions with **2**. Presumably interactions with PFS_{H5} or PFS_{H6} would be less detrimental as they are further removed from the actual aromatic ring. Interactions with TMS_{H3} might have greater effect by maintaining EGDMA in closer proximity to the TMS aromatic ring. Evaluation of interactions between the carbonyl oxygen of EGDMA and π -orbital of PFS did not reveal any increase in the density of EGDMA_{O5} in the presence of PFS_{C1}. Further evaluation of EGDMA interactions with TMS did however reveal small peaks in the density of EGDMA_{C3} and EGDMA_{C7}, 3.6 Å and 3.7 Å from TMS_{C1}, respectively (Figure 8). For the ethyl carbon, EGDMA_{C3}, this could have been a π - π type interaction with TMS whereas due to the lack of further functionality driving the increase in EGDMA_{C7} density it appears to have relied on weak London dispersion forces only. Although presumably weak in nature these interactions resulted in all EGDMA_{C3} within 4.0 Å of a TMS_{C1} for an average of 16.2 % of MD2 and all EGDMA_{C7} within 4.0 Å of a TMS_{C1} for an average 12.9 % of MD2. This high frequency of EGDMA in close proximity of the TMS π -orbital does have the potential to cause significant interference to π - π stacking interactions with **2**.

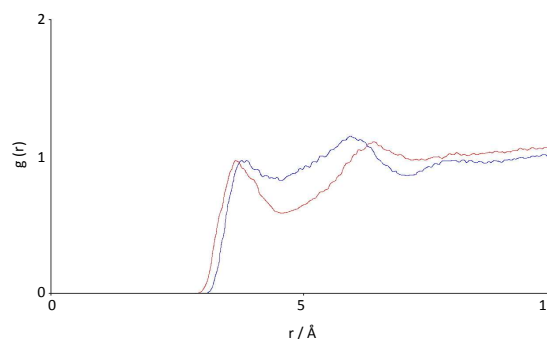


Figure 8. RDFs showing the density of EGDMA atoms as a function of the distance from TMS atoms during MD2. EGDMA_{C3}-TMS_{C1} (— trace) and EGDMA_{C7}-TMS_{C1} (— trace).

Competing Interactions – CL-T Interactions

In previous molecular dynamics studies templates, such as bupivacaine, have been observed to interact by hydrogen bonds with the carbonyl oxygen EGDMA.³¹ These interactions were predicted to increase the selectivity of the synthesised MIPs. For our systems **1**_{H1} and **2**_{H1} could potentially interact by hydrogen bonds with the carbonyl oxygen of EGDMA. Although **1**_{H1} and **2**_{H1} are not typical hydrogen bond donors their higher partial charges due to the electron withdrawing effects of the 5 chlorine substituents on **1** and 3 chlorine substituents on **2** was predicted to increase the stability of hydrogen bonds.

We calculated a RDF between **1**_{H1} and EGDMA_{O5} atoms during MD3 (Figure 9). This RDF indicated that interactions between **1** and EGDMA had transpired in hydrogen bond configurations by a small peak in the density of EGDMA_{O5} atoms 2.6 Å from atoms **1**_{H1} atoms. This distance is similar to the separation (1.9 Å) between bupivacaine and EGDMA observed in previous studies.³¹ Integration of this peak revealed that on average there was an EGDMA_{O5} within 3.1 Å of all **1**_{H1} for 10.0

% of MD3.

A RDF calculated between 2_{H1} atoms and EGDMA $_{\text{O5}}$ atoms during MD4 provided similar evidence for hydrogen bonds between **2** and EGDMA (Figure 9) by a small peak in the density of EGDMA $_{\text{O5}}$ atoms 2.6 Å from the 2_{H2} atoms. Integration of this peak indicated that these interactions were less frequent than the interactions between EGDMA and **1**. On average there was an EGDMA $_{\text{O5}}$ within 3.1 Å of all 2_{H2} for 8.5% of MD4. The lower frequency of interactions between **2** and EGDMA was attributed to the lower partial charge of 2_{H2} , than 1_{H1} , due to less chlorine substituents (3 versus 5).

Hydrogen bond interactions between the templates and EGDMA would have disrupted π - π stacking interactions between the templates and the FMs. The deleterious effects of these interactions were, however, dependent on the template and not the selection of FM. As **2** was observed to form π - π stacking interactions with PFS during MD4 template interactions with EGDMA were not attributed to the lack of π - π stacking interactions between **2** and TMS during MD2. Template interactions with EGDMA would have most likely increased the selectivity of the synthesised MIPs. This beneficial effect would have been greater for **1** than for **2** and this was attributed to higher partial charge of 1_{H1} than 2_{H2} .

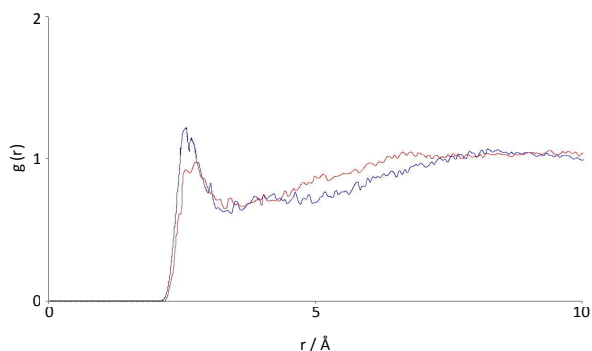


Figure 9. RDFs showing the density of EGDMA $_{\text{O5}}$ atoms as a function of the distance from 1_{H1} during MD3 (— trace) and 2_{H2} during MD4 (--- trace).

Conclusion

Molecular dynamics simulations were conducted of the pre-polymerisation mixtures used in the synthesis of **1** and **2** imprinted MIPs. Subsequent analysis revealed that the relative frequency of FM-T interactions within these simulated pre-polymerisation mixtures was consistent with results obtained by the synthesis and evaluation of the actual MIPs. The higher frequency of **1** interactions with TMS (54.7 % of MD1) than **1** interactions with PFS (44.7 %) corresponded to the higher IF (2.1) of **1** MIPs imprinted using TMS as the FM than the IF (1.7) of **1** MIPs imprinted using PFS as the FM. In addition, the higher frequency of PFS interactions with **2** (29.6 % of MD4) than TMS interactions with **2** (1.9 % of MD2) is consistent with the higher IF (3.7) of **2** MIPs imprinted using PFS as the FM than the IF (2.8) of **2** MIPs imprinted using TMS as the FM. TMS interactions with **1** dominated during MD1 due to the stronger interaction energy, whereas, due to weaker interaction energy with **2**, TMS interactions with **2** could not be maintained during MD2. The evaluation of FM interactions with other components of the pre-polymerisation mixture revealed that the cause for the lack of TMS interactions with **2** was, in part, due to interference caused by EGDMA interactions with TMS, which occurred between EGDMA $_{\text{C3}}$ and TMS $_{\text{C1}}$ for an average of 16.2 % of MD2 and between EGDMA $_{\text{C7}}$ and TMS $_{\text{C1}}$ for an average of 12.9 % of

MD2. The main reason was, however, attributed to MeOH interactions with TMS in both a hydrogen bond and perpendicular configuration. This positioned a MeOH directly above the π -orbital of all TMS for an average of 63.8% of MD2 creating significant interference to π - π stacking interactions between **2** and TMS.

While this body of work focuses on 1,2,3-trichlorobenzene (**2**) as a MIP template and PCB surrogate, our combined approach which spans EFP calculation and MD simulations with poorly functionalised MIP templates are directly applicable to other poorly functionalised MIP templates such as 2,4-dichlorophenoxyacetic acid;³⁶ benzo(a)pyrene;⁴¹ 1-hydroxypyrene;⁴² and 2,3,7,8-tetrachlorodibenzo-dioxin.⁴³ The EFP approach allows rapid and accurate determination of interaction energies of the most favourable FM-T interactions, and MD approaches allow rapid determination of any potential competing interactions that would ultimately impact on the quality and efficacy of the resulting MIP.

Experimental

Molecular dynamics simulations were performed using the AMBER version 8.0 suite of programs (UCSF, San Francisco, CA).⁴⁴

Preparation of a simulation began by entering the chemical structures for each type of pre-polymerisation component into the Amber antechamber program. The antechamber program then assigned the most appropriate set of molecular mechanics parameters to each atom of the pre-polymerisation components selected from the Amber99⁴⁵ and GAFF⁴⁶ force fields. Coulomb energy parameters required calculation of the partial charge of each atom, which was conducted by the AM1-BCC method.⁴⁷ Once parameters had been assigned the systems were built. PACKMOL software⁴⁸ was used to randomly the appropriate numbers of each pre-polymerisation component within an 80 x 80 x 80 Å box with periodic boundary conditions. Energy minimisations were then performed by 5000 steepest-descent and 5000 conjugate gradient steps to remove unfavourable contacts. The pre-polymerisation mixtures were then heated at constant volume from 0 to 273 K. A pressure of 1 bar was then applied to the box which was allowed to expand and contract in response to internal pressure until the pre-polymerisations mixtures had achieved a constant density. After confirming that the density of the pre-polymerisation mixture had stabilised, the dimensions of the box were fixed. A 5 ns production phase simulation then commenced with coordinates of the atoms recorded to a trajectory file every 2 ps.

Temperature and pressure were kept constant during the simulation by Langevin dynamics with a collision frequency of 1 ps⁻¹. A 9.0 Å cut-off was selected for the calculation of non-bonded interactions. The motion of hydrogen atoms were constrained using the SHAKE algorithm permitting a time step 0.002 ps.

After the completion of a simulation, interactions were analysed by calculation of the radial distribution function between pre-polymerisation components with a 0.05 Å bin size.

Acknowledgements

The authors thank Entech Industries (Australia) for financial support and Drs Clovia Holdsworth and Michael Bowyer for helpful discussions.

References

1. A. McCluskey, C. I. Holdsworth and M. C. Bowyer, *Org. Biomol. Chem.*, 2007, **5**, 3233.

2. A. Murray and B. Ormeci, *Environ. Sci. Pollut. Res. Int.*, 2012, **19**, 3820.
3. D. Yu, Y. Zeng, Y. Qi, T. Zhou and G. Shi, *Biosens. Bioelectron.*, 2012, **38**, 270.
- 5 4. A. Abouzarzadeh, M. Forouzani, M. Jahanshahi and N. Bahramifar, *J. Mol. Recognit.*, 2012, **25**, 404.
5. L. Schwarz, C. I. Holdsworth, A. McCluskey and M. C. Bowyer, *Aus. J. Chem.*, 2004, **57**, 759.
6. N. W. Turner, C. I. Holdsworth, S. W. Donne, A. McCluskey and M.C. Bowyer, *New J. Chem.*, 2010, **34**, 686.
- 10 7. K. Farrington, E. Magner and F. Regan, *Anal. Chim. Acta*, 2006, **566**, 60.
8. H. Kempe and M. Kempe, *Anal. Bioanal. Chem.*, 2010, **396**, 1599.
9. L. Ye, K. Yoshimatsu, D. Kolodziej, J. D. C. Francisco and E. S. Dey, *J. Appl. Polym. Sci.*, 2006, **102**, 2863.
- 15 10. Y. Diñeiro, I. Menéndez, C. Blanco-López, J. Lobo-Castañón, A. J. Miranda-Ordieres and P. Tuñón-Blanco, *Biosens. Bioelectron.*, 2006, **22**, 364.
11. C. I. Holdsworth, M. C. Bowyer, C. Lennard and A. McCluskey, *Aus. J. Chem.*, 2005, **58**, 315.
- 20 12. N. W. Turner, M. C. Bowyer, A. McCluskey and C. I. Holdsworth, *Aus. J. Chem.*, 2012, **65**, 1045.
13. K. Karim, F. Brenton, R. Rouillon, E. V. Piletska, A. Guerreiro, I. Chianella and S. A. Piletsky, *Adv. Drug Delivery Rev.*, 2005, **57**, 1795.
- 25 14. A. G. Mayes and M. J. Whitcombe, *Adv. Drug Delivery Rev.*, 2005, **57**, 1742.
15. K. -C. Ho, W. -M. Yeh, T. -S. Tung and J. -Y. Liao, *Anal. Chimica Acta*, 2005, **542**, 90.
- 30 16. N. Perez, M. Whitcombe and E. N. Vulson, *J. Appl. Polym. Sci.*, 2000, **77**, 1851.
17. E. Caro, N. Masque, R. M. Marce, F. Borrull, P. A. G. Cormack and D. C. Sherrington, *J. Chromatogr. A*, 2002, **963**, 169.
18. E. Turiel, E. Martin-Esteban, P. Fernández, C. Pérez-Conde and C. Cámara, *Anal. Chem.*, 2001, **73**, 5133.
- 35 19. J. Svenson, N. Zheng, U. Fohrman and I. Nicholls, *Ann. Lett.*, 2005, **38**, 227.
20. R. H. Schmidt and K. Haupt, *Chem. Mat.*, 2005, **17**, 1007.
21. G. Wulff, *Chem. Rev.*, 2002, **102**, 1.
- 40 22. *Polychlorinated Biphenyls Management Plan*. Australian Government, Department of the Environment, Water, Heritage and the Arts, 2002.
23. C. Baggiani, L. Anfossi, P. Baravalle, C. Giovannoli and G. Giraudi, *Anal. Bioanal. Chem.*, 2007, **389**, 413.
- 45 24. P. S. Reddy, T. Kobayashi and N. Fujii, *Eur. Polym. J.*, 2002, **38**, 779.
25. T. Kobayashi, P. S. Reddy, M. Ohta, M. Abe and N. Fujii, *Chem. Mater.*, 2002, **14**, 2499.
26. K. Yoshizako, K. Hosoya, Y. Iwakoshi, K. Kimata and N. Tanaka, *Anal. Chem.*, 1998, **70**, 386.
- 50 27. M. Lübke, M. J. Whitcombe and E. N. Vulson, *J. Am. Chem. Soc.*, 1998, **120**, 13342.
28. D. Cleland and A. McCluskey, *Org. Biomol. Chem.* 2013, **11**, 4646.
29. D. Cleland and A. McCluskey, *Org. Biomol. Chem.* 2013, **11**, 4672.
- 55 30. I. A. Kaliman and L. V. Slipchenko. *J. Comp. Chem.*, 2013, **34**, 2284.
31. B. C. G. Karlsson, J. O'Mahony, J. G. Karlsson, H. Bengtsson, L. A. Eriksson and I. A. Nicholls, *J. Am. Chem. Soc.*, 2009, **131**, 13297.
32. J. O'Mahony, B. C. G. Karlsson, B. Mizaikoff and I. A. Nicholls, *Analyst*, 2007, **132**, 1161.
- 60 33. G. D. Olsson, B. C. G. Karlsson, S. Shoravia, J. G. Wiklander and I. A. Nicholls, *J. Mol. Recognit.*, 2012, **25**: 69.
34. K. Golker, B. C. G. Karlsson, G. D. Olsson, A. M. Rosengren, I. A. Nicholls, *Macromol.*, 2013, **46**, 1408.
- 65 35. M. Sibrian-Vazquez and D. A. Spivak, *J. Am. Chem. Soc.*, 2004, **126**, 7827.
36. K. Haupt, A. Dzgoev and K. Mosbach. *Anal. Chem.* 1998, **70**, 628.
37. Y. Zhang, D. Song, L. M. Lanni and K. D. Shimizu. *Macromolecules*, 2010, **43**, 6284
- 70 38. Y. Zhang, D. Song, J. C. Brown and K. D. Shimizu. *Org. Biomol. Chem.* 2011, **9**, 120
39. E. C. Lee, B. H. Hong, J. Y. Lee, J. C. Kim, D. Kim, Y. Kim, P. Tarakeshwar and K. S. Kim, *J. Am. Chem. Soc.*, 2005, **127**, 4530.
40. J. Ran and P. Hobza, *J. Chem. Theory Comput.*, 2009, **5**, 1180.
- 75 41. J. Lai, R. Niessner and D. Knopp. *Anal. Chim. Acta* 2004, **522**, 137.
42. N. Kirsch, J. P. Hart, D. J. Bird, R. W. Luxton and D. V. McCalley. *Analyst* 2001, **126**, 1936.
43. K. Hosoya, Y. Watabe, T. Ikegami, N. Tanaka, T. Kubo, T. Sano and K. Kaya. *Biosens. Bioelectron.* 2004, **20**, 1185.
- 80 44. D. A. Case, T. E. Cheatham III, T. Darden, H. Gohlke, R. Luo, K. M. Merz Jr, A. Onufriev, C. Simmerling, B. Wang and R. J. Woods, *J. Comput. Chem.*, 2005, **26**, 1668.
45. J. Wang, P. Cieplak and P. A. Kollman, *J. Comput. Chem.*, 2000, **21**, 1049.
- 85 46. J. Wang, R. M. Wolf, J. W. Caldwell, P. A. Kollman and D. A. Case, *J. Comput. Chem.*, 2004, **25**, 1157.
47. A. Jakalian, D. B. Jack and C. I. Bayly, *J. Comput. Chem.*, 2002, **23**, 1623.
48. J. M. Martinez and L. Martinez, *J. Comput. Chem.*, 2003, **24**, 819.
- 90 ^a *Chemistry, Centre for Chemical Biology, The University of Newcastle, Callaghan, NSW 2308, Australia. Fax: +61 2 4921 5472; Tel: +61 2 4921 5472; E-mail: Adam.McCluskey@Newcastle.edu.au*
- ^b *Bioorganic and Biophysical Chemistry Laboratory, Linnæus University Centre for Biomaterials Chemistry, Linnæus University, Kalmar, SE-391 82 Kalmar, Sweden*
- ^c *Department of Chemistry-BMC, Uppsala University, Box 576, SE-751 23 Uppsala, Sweden*
- 100 † Electronic Supplementary Information (ESI) available: [details of any supplementary information available should be included here]. See DOI: 10.1039/b000000x/
- ‡ Footnotes should appear here. These might include comments relevant to but not central to the matter under discussion, limited experimental and
- 105 spectral data, and crystallographic data.